

GA-A25674

# **BERYLLIUM CAPSULE COATING DEVELOPMENT FOR NIF TARGETS**

by

**H.W. XU, C.S. ALFORD, J.C. COOLEY, L.A. DIXON, R.E. HACKENBERG,  
S.A. LETTS, K.A. MORENO, A. NIKROO, J.R. WALL, and K.P. YOUNGBLOOD**

**JANUARY 2007**



## **DISCLAIMER**

This report was prepared as an account of work sponsored by an agency of the United States Government. Neither the United States Government nor any agency thereof, nor any of their employees, makes any warranty, express or implied, or assumes any legal liability or responsibility for the accuracy, completeness, or usefulness of any information, apparatus, product, or process disclosed, or represents that its use would not infringe privately owned rights. Reference herein to any specific commercial product, process, or service by trade name, trademark, manufacturer, or otherwise, does not necessarily constitute or imply its endorsement, recommendation, or favoring by the United States Government or any agency thereof. The views and opinions of authors expressed herein do not necessarily state or reflect those of the United States Government or any agency thereof.

# BERYLLIUM CAPSULE COATING DEVELOPMENT FOR NIF TARGETS

by

H.W. XU, C.S. ALFORD,\* J.C. COOLEY,<sup>†</sup> L.A. DIXON, R.E. HACKENBERG,\*  
S.A. LETTS,\* K.A. MORENO, A. NIKROO, J.R. WALL, and K.P. YOUNGBLOOD

This is a preprint of a paper presented at the 17th Target Fabrication Specialist Meeting, San Diego, California on October 1-5, 2006 and to be published in *Fusion Science and Technology*.

\*Lawrence Livermore National Laboratory, Livermore, California.

<sup>†</sup>Los Alamos National Laboratory, Los Alamos, New Mexico.

Work supported by  
the U.S. Department of Energy  
under DE-AC52-06NA27279, W-7405-ENG-48, and W-7405-ENG-36

GENERAL ATOMICS PROJECT 30272  
JANUARY 2007



## BERYLLIUM CAPSULE COATING DEVELOPMENT FOR NIF TARGETS

H.W. Xu,<sup>1</sup> C.S. Alford,<sup>2</sup> J.C. Cooley,<sup>3</sup> L.A. Dixon,<sup>1</sup> R.E. Hackenberg,<sup>3</sup> S.A. Letts,<sup>2</sup> K.A. Moreno,<sup>1</sup>  
A. Nikroo,<sup>1</sup> J.R. Wall,<sup>1</sup> and K.P. Youngblood<sup>1</sup>

<sup>1</sup>General Atomics, P.O. Box 85608, San Diego, California 92186-5608

<sup>2</sup>Lawrence Livermore National Laboratory, P.O. Box 808, Livermore, CA 94550

<sup>3</sup>Los Alamos National Laboratory, P.O. Box 1663, Los Alamos, NM 87545  
xuh@fusion.gat.com

*Various morphologies have been observed in sputter-deposited Be ablator capsules, including nodular growth, cone growth and twisted grain growth. By devising an agitation method that includes both bouncing and rolling the spherical mandrels during deposition, and by reducing the coating rate, consistent columnar grain structure has now been obtained up to 170 mm. Low mode deformation of the shells is observed on thin CH mandrels, but is suppressed if stiffer mandrels are used. Ablator density measured by weighing and x-ray radiography is 93%–95% of bulk density of Be. Transmission electron microscopy shows 100–200 nm size voids in the film and striations inside the grains. Be shells produced with rolling agitation have met most of the NIF specifications. Some of the few remaining issues will be discussed.*

## I. INTRODUCTION

A graded copper-doped beryllium capsule is the current NIF<sup>1</sup> point design<sup>2</sup> for ignition in 2010. The point design sets a series of specifications for the capsules to meet, which include coating density, void defect size and volume, outer and inner surface roughness, x-ray optical depth uniformity and impurity levels. Figure 1 shows current 1 MJ design multilayer composition [Fig. 1(a)] and inner/outer surface roughness specifications [Fig. 1(b)].

Be coatings on spherical surfaces have been developed at Lawrence Livermore National Laboratory (LLNL) and later at General Atomics (GA) for the production of Be capsules using a magnetron sputtering technique.<sup>3-9</sup> Previous and current efforts have focused on improving Be coating density and getting uniform and consistent microstructures in order to develop dense material, smooth inner and outer surfaces, and leak-free

NIF capsules. Briefly, Be coatings were produced by sputtering Be onto CH mandrels<sup>10</sup> placed in a pan with bouncing agitation. As pointed out in previous papers,<sup>8,9</sup> Be coatings produced in this way exhibit a variety of growth modes, such as nodular growth and twisted grain structure, and they typically have low densities. The measured surface roughness increases with coating thickness.<sup>8</sup> Although the outer surface can be polished to NIF specifications,<sup>11</sup> a smooth growth front surface is desired because it leads to a smooth interface between layers, which will improve optical depth uniformity. Be capsules are normally obtained by removing the CH mandrels through a laser drilled hole at 400°-550°C in air. The remaining Be shells are used for gas retention tests and trace element analysis, which will be discussed elsewhere.<sup>12-13</sup>

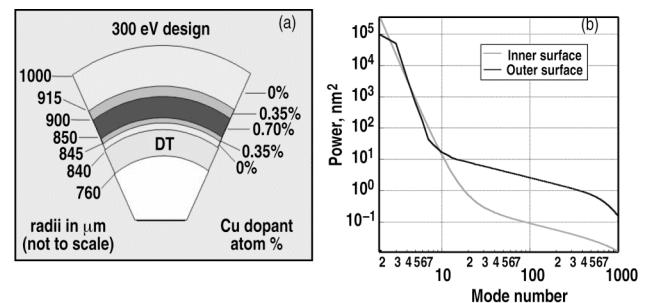


Figure 1. (a) Current NIF 1MJ design of graded Cu doped Be capsule. (b) Capsule inner and outer surface roughness specifications. The horizontal axis is mode number and the vertical axis is the power of the surface roughness.

We report our progress in improving Be coating quality for getting a more uniform and denser Be coating. We will also compare our current full-thickness Be capsules with NIF specifications to show where the capsules are meeting specifications. Some of the remaining issues that must be resolved to meet all NIF

specifications will be discussed, and the direction of future experimental work will be proposed.

## II. EXPERIMENTAL

Be coatings were prepared at working pressures of Ar between 3 mTorr and 10 mTorr in a high vacuum chamber with a base pressure of  $1 \times 10^{-6}$  torr evacuated by a cryopump. A typical set-up includes three 2 in. magnetron guns for sputtering Be, and one 1.3 in. magnetron gun for sputtering Cu. The mandrels are normally glow discharge polymer (GDP) shells<sup>10</sup> agitated in a bouncing pan under the sputtering guns to uniformly coat the shells. The details of the Be coating process can be found in earlier publications.<sup>8,9</sup> Some other types of mandrels, such as Si and Ni beads, were also used for the purpose of obtaining better surface finish and exploring different methods of mandrel removal.

Bouncing agitation was used previously with the intent of getting uniform coating on shells. However, as described in previous publications, coatings obtained in this way generally showed low density and poor microstructure. In order to improve the coating microstructure, we changed agitation from bouncing to rolling.<sup>14</sup> With less aggressive rolling agitation, during the beginning of a run shells sometimes stick together due to static charge. To avoid this we incorporate rolling with tapping or gentle bouncing with the rolling. With this approach we obtained microstructures which were more uniform than previously observed. Other undesirable modes of growth were also suppressed, as described below.

The density of the coating was measured by mass per volume. To get the volume, the shell diameter and thickness were measured by x-ray radiography. The mass of the shells were measured using an ATI Cahn C-35 microbalance accurate to 0.3  $\mu\text{g}$ . The weight of the beryllium-coated shells is typically  $\sim 2$  mg or higher, which translates into an error in density due to weighing that is well below 0.1%. The accuracy of diameter measurements using x-ray radiography is  $\sim 1$   $\mu\text{m}$ , introducing an error of only  $\sim 0.1\%$  in the density measurements. The thickness measurement contributes the most error to the density measurements. The thickness is typically measured using radiography which can have an error of as much as  $\pm 1$   $\mu\text{m}$ , with the associated error of  $\pm 2\%$  in the density.

Cu-doping was performed by co-sputtering Be and Cu to test our capability of controlling the Cu doping levels for meeting the NIF Cu doping profile specification. The Cu concentration was obtained from radiograph measurements.<sup>15</sup> The full thickness shell with

graded Cu doped layers was produced according to coating rates calibrated for pure Be and Cu doped Be. Thickness and doping concentration are generally controlled within  $\pm 10\%$ .

The microstructure and defects in the coatings were characterized by scanning electron microscopy (SEM) and transmission electron microscopy (TEM). The voids in the coating were observed by TEM images from which their sizes were estimated. The surface roughness was measured by AFM spheremapper<sup>16</sup> and optical depth uniformity was measured by precision radiography.<sup>17</sup>

## III. RESULTS

In our previous publications, we have shown that when using bouncing agitation with a high coating rate, the film microstructure showed twisted columnar structure with low density.<sup>9</sup> However, when the agitation was changed to rolling, and the coating was made at lower deposition power as in the current work, the resulting microstructure showed a uniform columnar structure. Figure 2 shows SEM cross-sections of (a) a twisted structure obtained at higher coating power (300 W,  $\sim 1.5$   $\mu\text{m}/\text{h}$ ) with bouncing agitation and (b) a uniform columnar structure deposited at lower power (100 W,  $\sim 0.4$   $\mu\text{m}/\text{h}$ ) with rolling agitation. The twisted structure in Fig. 2(a) is less dense ( $\sim 80\%$  of Be bulk density) than the structure in Fig. 2(b) ( $\sim 95\%$  of Be bulk density). It is seen from Fig. 2(a) that the twisted structure has columns oriented along different directions, while only columns along radial directions are observed in the uniform columnar structure in Fig. 2(b). A few factors may have contributed to the differences in microstructure and density of these two films: the coating rates, the sputtering power levels and the agitation type. The higher sputtering power level has been shown to introduce local heating and result in gas rarefaction effects, which can increase the sputtered atom mean free path within the deposition chamber.<sup>18</sup> Rolling agitation, especially as the shells become heavier, normally leads to a smoother surface due to gentle polishing effects. The details of the formation mechanisms of the observed microstructure require further studies.

The density of the coating was measured to determine if it changes with coating thickness and deposition conditions. Figure 3 shows a plot of the measured density of Be coatings versus the coating thickness. Within the measurement error range of  $\pm 2\%$ , the results show that the coating density is independent of the coating thickness with an average value of  $\sim 95\%$  of bulk density. No measurable density change was observed for the films when the Ar pressure was varied from

3 mTorr to 10 mTorr. These Be coatings have met the NIF density requirements of  $95\% \pm 3\%$  of bulk density.

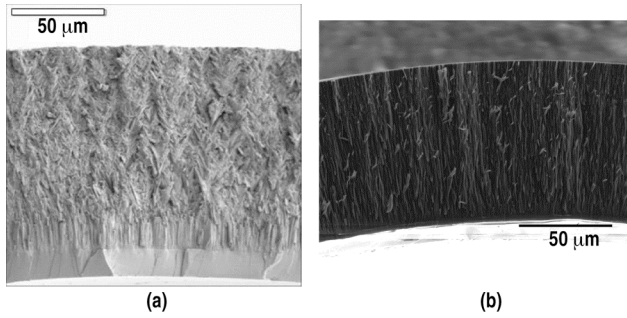


Figure 2. (a) Twisted structure observed at 300 W coating power with bouncing agitation. (b) Uniform columnar structure for a 144  $\mu\text{m}$  Be film obtained at 100 W coating power with rolling agitation.

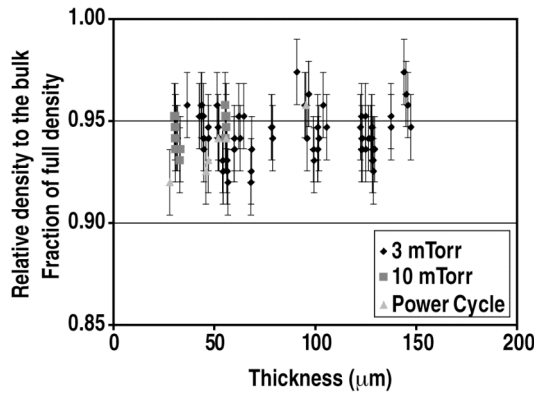


Figure 3. A plot of measured density of Be coatings versus coating thickness at different processing Ar pressures.

Using TEM we have compared the defects in low density coatings made at higher coating power (3 guns at 300 W per gun) and bouncing agitation with our recent higher density coatings made at lower coating power (3 guns at 100 W per gun) and rolling agitation. Figure 4(a) shows voids (white features) with lateral dimensions larger than 500 nm for a previous coating with  $\sim 80\%$  of Be bulk density. The regions with different grey scales are differently oriented grains. Figure 4(b) shows small voids along domain boundaries with lateral dimensions of less than 200 nm for a recent coating of  $\sim 95\%$  of Be bulk density. In addition to the small scattered voids, some fine intra-granular striation lines were also observed in this sample. The NIF specification states that the void size must be less than  $0.1 \mu\text{m}^3$ , which corresponds to a lateral dimension of  $\sim 500 \text{ nm}$ . Numerous samples prepared by sputtering have been analyzed by TEM and all of them met the NIF void specification.

Precision radiography was performed on a  $125 \mu\text{m}$  thick sputtered Be shell as a first step to understand the optical depth uniformity of Be shells.<sup>17</sup> The measured optical depth fluctuation is lower than the NIF specification curve, except at  $\sim$  mode 2. For this shell the uniformity was very close to meeting the specification. However, this measurement was done on a pure Be shell. Further investigation is necessary of a full-thickness graded Cu-doped Be shell in order to fully determine the optical depth uniformity of NIF-design Be shells.

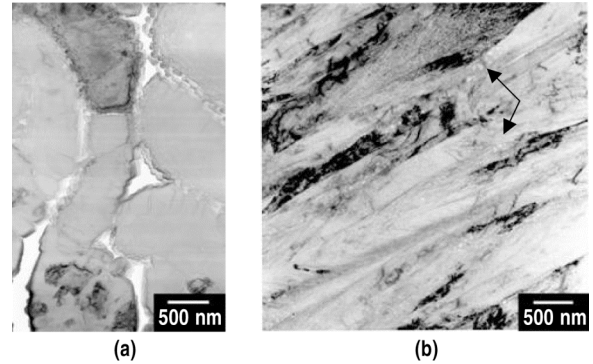


Figure 4. (a) TEM image of Be coating at higher coating power with bouncing agitation. Voids  $>500 \text{ nm}$  in dimension are visible in this image. (b) TEM image of Be coating done at lower coating power with rolling agitation. The scattered voids still exist ( $<200 \text{ nm}$ ) in the coating; and they are barely visible along the columnar grain boundaries (a few voids were pointed by the arrows).

To test our coating thickness and concentration control, full thickness NIF design graded Cu-doped Be shells were fabricated. The coating was produced by using three Be guns and one Cu gun with rolling agitation. The results are shown in Table I where the measured shell layer thicknesses and Cu concentrations are compared with the NIF specifications. The Cu concentrations at each of the layers meet the NIF graded Cu-doped Be shell design specifications. By controlling the gun power and deposition time, the layer thickness and doping level can be achieved to within  $\sim 10\%$  of the targeted values. The deviation from the targeted values can be attributed to small, but acceptable variation in coating rates.

It has been observed that the Be shell surface roughness in the middle modes is impacted by the mandrels used. Be coatings on thin CH mandrels ( $\sim 10\text{-}20 \mu\text{m}$ ) resulted in low-mode wrinkling. In Fig. 5 the grey line is a plot of the surface roughness of a full thickness shell deposited on a thin CH mandrel. The dark line represents the NIF specification of the surface roughness for the graded Cu-doped design. The shell surface roughness follows NIF specification closely except

around mode 10. From the AFM traces (not shown), one can see that these modes appear as low-mode “wrinkling.” Generally, high-mode roughness can be polished to below NIF specifications.<sup>11</sup> However, low mode surface roughness can not be removed by polishing because the shell wall thickness uniformity is sacrificed when the low mode surface roughness is removed for uniform thickness shells. If stiffer mandrels are used, such as Si beads, the low mode surface roughness can be improved. The light grey line in Fig. 5 shows the surface roughness of a Be coating on a Si bead. The low mode surface roughness is below NIF curve, which indicates that sputtered Be by itself is not the cause of low mode surface roughness. The possible use of bead mandrels, as well as thicker CH mandrels, is discussed in a paper in this issue by S. Bhandarkar et al.<sup>19</sup>

Table I. A Comparison of a Full Thickness NIF Design Graded Cu-doped Be Shell to the NIF Specifications

| Composition/<br>Thickness                | NIF<br>Specifications | Measured on<br>Full Thickness<br>Graded<br>Cu-Doped<br>Be Shell |
|--|-----------------------|---|
| 1st layer thickness<br>( $\mu\text{m}$ ) | Be: $6\pm 1$          | Be: 6   |
| 2nd layer thickness<br>( $\mu\text{m}$ ) | Be(Cu): $5\pm 1.5$    | Be(Cu): 5   |
| 2nd layer Cu<br>concentration (%)        | 0.35—0.1              | 0.37  |
| 3rd layer thickness<br>( $\mu\text{m}$ ) | Be(Cu): $50\pm 3$     | Be(Cu): 48.9  |
| 3rd layer Cu<br>concentration (%)        | $0.7\pm 0.05$         | 0.66  |
| 4th layer thickness<br>( $\mu\text{m}$ ) | Be(Cu): $14\pm 3$     | Be(Cu): 13.6  |
| 4th layer Cu<br>concentration (%)        | $0.35\pm 0.1$         | 0.37  |
| Total thickness ( $\mu\text{m}$ )        | $160\pm 1.5$          | 160.5   |

The measurement of the inner surface roughness is a destructive measurement done by breaking the shell and analyzing the inside surface of the resulting shards using spherical interferometry.<sup>20</sup> From this interferometry data, the inner surface roughness power spectrum for a sample shell was determined and is shown in Fig. 6. Due to the limited range of the spherical interferometer, the surface roughness data only covers modes larger than 120. The plot in Fig. 6 shows that the inner surface roughness in the measured range met the NIF specification.

One of the remaining issues for Be shells to fully meet the NIF specifications is to measure the trace element concentration, which affects the opacity of the shell. It has been observed that as-deposited Be shells

have x-ray absorption very close to the NIF specification.<sup>13</sup> The main trace element is oxygen which is normally measured at  $\sim 1$  at% in as-deposited Be shells. The oxygen was mainly introduced by the oxide in Be targets and exposure to air after the Be shells were removed from the vacuum chamber. However, to remove the GDP mandrel, Be shells have to be laser drilled and then heated in air at  $400^{\circ}\text{--}500^{\circ}\text{C}$  for 60 h.<sup>21</sup> It was found that after mandrel removal, the Be shells picked up a significant amount of oxygen, resulting in x-ray absorption levels higher than allowed by the NIF specification, as shown in Fig. 7. The plot shows that even at  $100^{\circ}\text{C}$  there is significant oxygen pick-up.

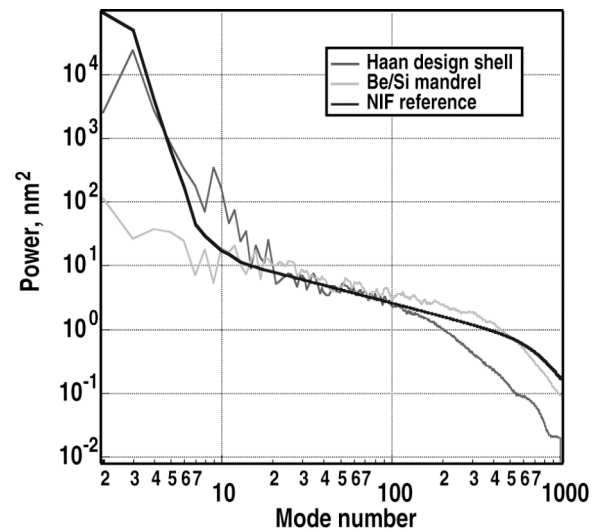


Figure 5. Plots of Be shell outer surface roughness on a thin GDP mandrel and on a Si bead compared to the NIF specifications. The grey line is for surface roughness on a thin GDP mandrel, the light grey line is on a Si bead. The dark line is a NIF specification curve (Haan Design).

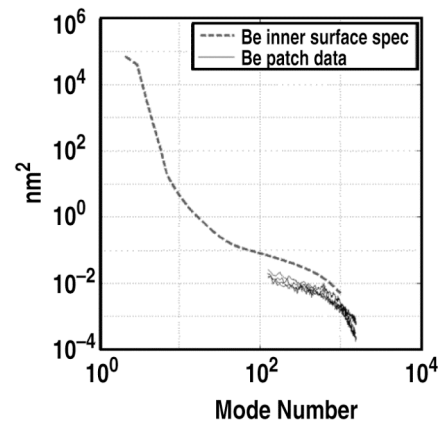


Figure 6. The inner surface roughness power spectrum obtained from spherical interferometry data.

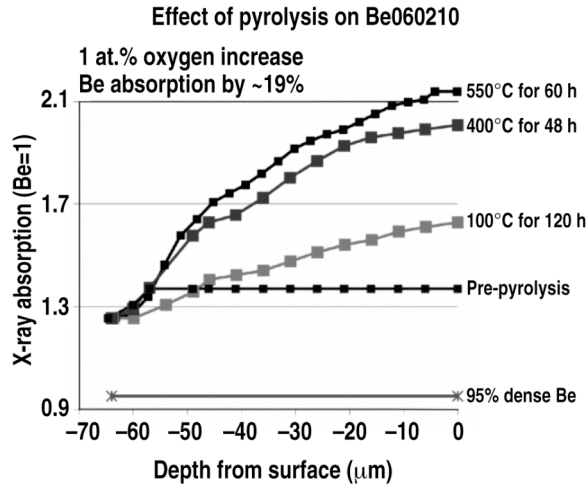


Figure 7. Plot of x-ray absorption of Be shells (which relates directly to the oxygen concentration) after heated at different temperatures for extended periods. Significant oxygen pick-up was observed above 100°C. The plot is from outer surface to inner surface measured by x-ray radiography.

One proposed solution to reduce oxygen pick-up is to use thin Be mandrels. Thin Be mandrels can be made by coating CH mandrels with a thin Be layer (a few microns) and then removing the CH mandrels using the regular mandrel removal process.<sup>21</sup> The remaining thin Be mandrels will have higher oxygen pick-up. However, the Be shells deposited on thin Be mandrels will not need to go through the mandrel removal process. Therefore, higher oxygen pick-up will be limited to the thin Be mandrel layer and the oxygen pick up through the entire thickness of the 160  $\mu\text{m}$  Be shells will be minimized.

Another important issue for Be shells is fuel gas retention. Be shells produced by sputter coating had a very short gas retention half-life, from a few minutes to a few hours. We have recently developed a Be:B permeation barrier which dramatically improves the gas retention half life of these shells. This work will be discussed in a separate paper in this issue.<sup>12</sup>

#### IV. SUMMARY

Be shells with consistent microstructures have been developed for NIF capsule applications. The Be coatings have repeatedly shown 93%-95% of bulk density, which meets the NIF specification for density. The voids in the coatings were studied by TEM in numerous samples and all met the NIF specifications for the void volume. Preliminary precision radiography measurements on a 125  $\mu\text{m}$  Be shell indicate that the shell was close to

meeting the NIF specification on optical depth uniformity. The Cu dopant profile of Be shells shows that the doping level can be controlled within the NIF requirement. Be coating on thin GDP mandrels showed some middle mode wrinkling which has been improved by using stiffer mandrels such as Si beads. Inner surface roughness has been measured by spherical interferometry on shards of broken shells and those limited data meets the NIF specification for the inner surface roughness. The remaining issues of oxygen pick-up during mandrel removal and gas tight shells have promising solutions based on thin Be mandrels and thin Be:B permeation barrier layers in the first micron of coating.

#### ACKNOWLEDGMENT

This work was performed under the auspices of the U.S. Department of Energy by General Atomics under DE-AC52-06NA27279, by the University of California Lawrence Livermore National Laboratory under W-7405-Eng-48, and by Los Alamos National Laboratory under W-7405-ENG-36. The authors acknowledge GA staff members H. Huang for doing x-ray radiograph analysis of Cu doping profiles, oxygen pick-up and patch analysis of spherical interferometer data, S. Eddinger for carrying out precision x-ray radiograph measurement of optical depth uniformity, T. Lee for providing spherical interferometry data, and J. Gibson for providing AFM spheremapping data. The authors are also pleased to acknowledge useful conversations with S. Bajt, J. Taylor, and R. McEachern of LLNL about various aspects of this work, as well as R. Cook of LLNL and H. Wilkens of GA for their help in putting this manuscript together.

#### REFERENCES

1. G. H. MILLER, E. I. MOSES, and C. R. WUEST, "The National Ignition Facility," *Opt. Eng.* **43**, 2841 (2004).
2. S. W. HAAN, M. C. HERRMANN, P. A. AMENDT, D. A. CALLAHAN, T. R. DITTRICH, M. J. EDWARDS, O. S. JONES, M. M. MARINAK, D. H. MUNRO, S. M. POLLAIN, J. D. SALMONSON, B. K. SPEARS, L. J. STUTER, "Update on Specifications for NIF Ignition Targets, and Their Rollup into an Error Budget," *Fusion Sci. Technol.* **49**, 553 (2006).
3. R. J. BURT, S. F. MEYER, and E. J. HSIEH, "Radio Frequency Magnetron Sputtering of Thick Film Amorphous Beryllium," *J. Vac. Sci. Technol.* **17**, 407 (1980).

4. E. J. HSIEH, C. W. PRICE, E. L. PIERCE, and R. G. WIRTENSON, "Effects of Nitrogen Pulsing on Sputter-Deposited Beryllium Films," *J. Vac. Sci. Technol.* **A8**, 2165 (1990).
5. R. MCEACHERN, C. ALFORD, R. COOK, D. MAKOWCKI, and R. WALLACE, "Sputter-Deposited Be Ablators for NIF Target Capsules," *Fusion Technology* **31**, 435 (1997).
6. R. McEACHERN and C. ALFORD, "Evaluation of Boron-doped Beryllium as an Ablator for NIF Target Capsules," *Fusion Technol.* **35**, 115 (1999).
7. R. McEACHERN, C. ALFORD, R. COOK, D. MAKOWCKI, and R. WALLACE, "Sputter-Deposited Be Ablators for NIF Target Capsules," *Fusion Technol.* **31**, 435 (1997).
8. H. W. XU, A. NIKROO, J. R. WALL, R. DOERNER, M. BALDWIN, and J. H. YU, "Be Coating on Spherical Surface for NIF Target Development," *Fusion Sci. Technol.* **49**, 778 (2006).
9. M. MCELFRISH, J. GUNTHER, C. ALFORD, E. FOUGHT, R. COOK, A. NIKROO, H. XU, J. C. COOLEY, R. D. FIELD, R. E. HACKENBERG, and A. NOBILE, "Fabrication of Beryllium Capsules with Copper-Doped Layers for NIF Targets: a Progress Report," *Fusion Sci. Technol.* **49**, 786 (2006).
10. B. W. MCQUILLAN, A. NIKROO, D. A. STEINMAN, F. H. ELSNER, D. G. CZECHOWICZ, M. L. HOPPE, M. SIXTUS, and W. J. MILLER, "The P $\alpha$ MS/GDP Process for Production of ICF Target Mandrels," *Fusion Technol.* **31**, 381 (1997).
11. M. L. HOPPE and E. CASTILLO, "Polishing of Beryllium Capsules to Meet NIF Specifications," *J. Phys. IV France* **133**, 895 (2006).
12. A. NIKROO, et al., "Investigation of Deuterium Permeability of Sputtered Beryllium and Graded Copper Doped Beryllium Shells," *Fusion Sci. Technol.*, this issue.
13. H. HUANG, et al. "Quantitative Radiography: Film Model Calibration and Dopant/Impurity Measurement in ICF Targets," *Fusion Sci. Technol.*, this issue.
14. C. C. ROBERTS, P. J. ORTHION, A. E. HASSEL, B. K. PARRISH, S. R. BUCKLEY, E. FEARON, S. A. LETTS and R. C. COOK, "Development of Polyimide Ablators for NIF: Analysis of Defects on Shells, a Novel Smoothing Technique and Upilex Coatings," *Fusion Technol.* **38**, 94 (2000).
15. H. HUANG, R. B. STEPHENS, S. A. EDDINGER, J. GUNTHER, A. NIKROO, K. C. CHEN, H. W. XU, "Nondestructive Quantitative Dopant Profiling Technique by Contact Radiography," *Fusion Sci. Technol.* **49**, 650 (2006).
16. H. HUANG, R. B. STEPHENS, J. B. GIBSON, and I. VALMIANSKI, "3D Surface Reconstruction of ICF Shells after Full Surface Spheremapping," *Fusion Sci. Technol.* **49**, 642 (2006).
17. S. EDDINGER, et al., "Measuring Optical Depth Variations in NIF Shells," *Fusion Sci. Technol.*, this issue.
18. S. M. ROSSNAGEL, "Gas Density Reduction Effects in Magnetrons," *J. Vac. Sci. Technol.* **A6**, 19 (1988).
19. S. BHANDARKAR, et al. "Removal of the Inner Mandrel from Sputter Coated Capsules for NIF Targets," *Fusion Sci. Technol.*, this issue.
20. R. C. MONTESANTI, M. A. JOHNSON, E. R. MAPOLES, D. P. ATKINSON, J. D. HIGHERS, and J. L. REYNOLDS, "Phase-shift Diffraction Interferometer for Inspecting NIF Ignition-Target Shells," *American Society for Precision Engineering Annual Conference Proceedings*, 2006.
21. R. C. COOK, S. A. LETTS, S. BUCKLEY, and E. FEARON, "Pyrolytic Removal of the Plastic Mandrel from Sputtered Beryllium Shells," *Fusion Sci. Technol.* **49**, 802 (2006).